

Bark Frequency Spectrum in Parallel-form Remote Active Noise Control

Muhammad Waqas Munir* and Waleed H. Abdulla

Department of Electrical, Computer and Software Engineering

The University of Auckland, Auckland, New Zealand

E-mail: (M.Waqas, W.Abdulla)@auckland.ac.nz

Abstract—Active noise control (ANC) is widely used to reduce low-frequency noises. ANC aims to cancel the noise by generating another noise with equal magnitude and opposite phase. The superposition of the noise and anti-noise cancel out each other to create a zone of quiet (ZoQ) at an error microphone. However, in case of physical limitations or application constraints to place the error microphone, the virtual sensing algorithms are used to cancel the unwanted noises at the desired location. In many practical ANC applications, the primary noise contains multiple discrete low frequencies. A narrowband active noise control structure is often applied to reduce unwanted noise when the multiple tones have proximity frequencies. In this paper, a parallel-form remote ANC algorithm is proposed to cancel the narrowband noises at the remote location. A parallel-form ANC structure separates the discrete frequencies into a series of adaptive filters. Then delayless bandpass filter bank is used to split the measured error signal, and use the individual error signal to update the corresponding adaptive filters. The transfer function of the remote controller is derived in the acoustic domain, which moves the ZoQ from the error microphone to the nearby remote location. Computer simulations are performed to verify the performance of the proposed algorithm.

I. INTRODUCTION

Active noise control (ANC) is an efficient technique to reduce low-frequency noises, where conventional passive methods are costly, bulky, and ineffective for many industrial applications. Active noise control is based on the simple principle of destructive interference. The superposition of two sound fields that have an equal amplitude but opposite phase, cancel out each other and create a small zone of quiet (ZoQ). In real-world, vibrating machines or reciprocating and rotary motion devices generate plenty of noxious noises that mostly have discrete low frequencies. The parallel-form narrowband active noise control (NANC) has been found effective and efficient to diminish the narrowband noise with distinct frequencies.

The parallel-form narrowband ANC system with a least mean square (LMS) algorithm was investigated and developed by several researchers [1-3]. However, these parallel-form narrowband ANC algorithms update all adaptive filters using the same error signal. Thus the residual noise component from other channels disturb the adaptive algorithm of each filter. To obtain the individual error signals for corresponding channels, Yang et al. has proposed a parallel-form narrowband ANC structure using multiple notch filters [4-5]. However, it ignores the problem of additional secondary path delay introduced by the notch filters. In [6], Xiao proposed a

narrowband ANC system with multiple parallel filters and an additional bandpass filter bank to decompose the output of each filter. This method uses the same error signal to update all adaptive filters. However, it still incur a problem similar to the parallel form model. The performance of narrowband ANC degrades when the error signal does not approach to zero in all the components. Later, in [7-9] Chang and Kuo proposed complete direct/parallel narrowband algorithms, that use the delayless bandpass filter bank to split the residual error signal into independent channels. Then the cost function of the adaptive algorithm is updated by the corresponding individual error signal based on the frequency components of the input signal. The complete NANC structures have been further investigated and implemented in various ANC architectures such as feedback ANC [10] and variable leaky LMS [11] algorithms.

Those conventional complete parallel-form narrowband ANC algorithms create a ZoQ by minimizing the acoustic pressure at the error sensor location. However, for some ANC applications, there are some physical or application constraints to place physical error sensors at the desired location. To overcome this problem, several virtual or remote sensing algorithms have been developed [12-16]. Therefore, to achieve the noise attenuation and to introduce more flexible positioning of the ZoQ, the conventional parallel-form NANC algorithm needs to be amended. Virtual sensing techniques can be used in parallel-form NANC algorithms to achieve the noise attenuation at the desired location.

The motivation of this paper is to develop a parallel-form remote ANC algorithm that can cancel the unwanted narrowband noises at the remote location. At the same time, the physical error microphone remains untouched. In our proposed algorithm a parallel-form remote ANC structure separate the discrete frequencies into a series of adaptive filters. Then each adaptive filter works independently with a single frequency of Bark frequency spectrum and its corresponding remote adaptive controller. The transfer function of the remote adaptive controller for each frequency component is derived through the wave equation in the acoustic domain. Using multiple delayless bandpass filters, the error signal is divided into different channels depending on the frequency components of the input signal. Therefore, the individual error signal updates the corresponding adapting filter containing the same frequency component as in the input signal.

The rest of the paper is organized as follows. Section II introduces the parallel-form narrowband ANC system. The acoustic modeling of the remote adaptive controller is shown in section III, while section IV describes the proposed parallel-form remote ANC algorithm. Section V summarizes the simulation results and discuss the performance of the proposed algorithm, and the conclusion is drawn in section VI.

II. PARALLEL-FORM NARROWBAND ANC SYSTEM

The parallel-form narrowband ANC system separates the frequency components of the input signal into multiple channels connected in parallel. The complete structure of the parallel-form NANC system is illustrated in Fig. 1. The bandpass IIR filters are used to split the frequency components into multiple parallel channels, and each channel consists of an independent sinusoidal reference signal $x_i(n)$, and the adaptive FIR filter $W_i(z)$ with an adaptive algorithm FxLMS. The outputs of these adaptive filters are summed together to a singular secondary path and generates a single canceling signal $y(n)$. Then in the feedback path of the adaptive algorithm, a bank of bandpass IIR filters $B_i(z)$ ($i = 1, \dots, M$) are used to split the error signal for generating independent error signals to their corresponding input frequencies $e_i(n)$, $i = 1, \dots, M$. These bandpass filters are delayless, and they will not produce an extra delay between their input signal $e(n)$ and output signals $e_i(n)$. The bandpass filters are delayless for the narrowband signal at the center frequency of passband. This section describes an overall structure of a parallel-form narrowband system. However, the complete modeling of chosen delayless filters is described in [7]. As shown in Fig. 1, the bandpass IIR filters are used to separate the frequency components of the reference signal $x_i(n)$ at frequency f_i expressed as;

$$x_i = \cos(2\pi f_i n), \quad i = 1, 2, \dots, M. \quad (1)$$

These separated signals are used as a reference input of the adaptive filters $W_i(z)$ connected in parallel. The error signals of these adaptive filters are used to update the filtered-x LMS (FxLMS) algorithm. The output signal of i th adaptive filter $y_i(n)$ is

$$y_i(n) = \sum_{l=0}^{L-1} w_{i,l}(n)x_i(n-l) = \mathbf{w}_i^T(n)\mathbf{x}_i(n) \quad (2)$$

where $w_{i,l}$ is the coefficients of the adaptive filter $W_i(z)$ of length L . The weight vector $\mathbf{w}_i(n)$ and input vector $\mathbf{x}_i(n)$ are given as

$$\mathbf{w}_i(n) = [w_{i,0}(n) \ w_{i,1}(n) \ \dots \ w_{i,L-1}(n)]^T \quad (3)$$

$$\mathbf{x}_i(n) = [x_i(n) \ x_i(n-1) \ \dots \ x_i(n-L+1)]^T \quad (4)$$

and T represent the transpose operation. The canceling signal $y(n)$ is the combination of the output of the M adaptive filters.

$$y(n) = \sum_{i=1}^M y_i(n) \quad (5)$$

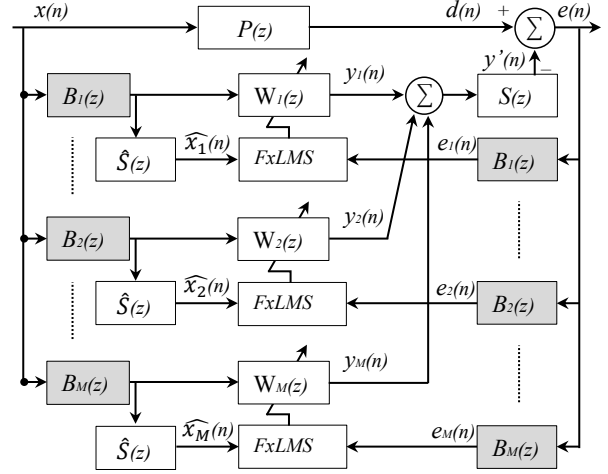


Fig. 1: Block diagram of parallel-form FxLMS

The FxLMS algorithm for updating the weights of the adaptive FIR filter can be expressed as,

$$\mathbf{w}_i(n+1) = \mathbf{w}_i(n) + \mu_i e_i(n) \hat{\mathbf{x}}_i(n) \quad (6)$$

Where μ_i is the adaption step-size of the i th adaptive filter, and $\hat{x}_i(n)$ is the filtered reference signal of the input $x_i(n)$.

$$\hat{x}_i(n) = \hat{s}_i(n) * x_i(n) \quad (7)$$

Where $s_i(n)$ and $\hat{s}_i(n)$ are the coefficient of the i th order secondary path $S(z)$ and the estimated secondary path $\hat{S}(z)$ respectively. As per the input signal $x(n)$ defined in (8), the bandpass filters separate its M individual frequency signals

$$x(n) = \sum_{i=1}^M x_i(n) \quad (8)$$

The primary noise $d(n)$ can be expressed as the sum of M frequency components.

$$d(n) = \sum_{i=1}^M d_i(n) \quad (9)$$

Where, $d_i(n)$ have the frequency components similar to $x_i(n)$. Since, each adaptive filter $W_i(z)$ is a linear FIR filter, the noisy signal error; $e(n)$, can be decomposed into multiple frequency components

$$e(n) = \sum_{i=1}^M e_i(n) \quad (10)$$

Where, $e_i(n)$ contains the same frequency components as $x_i(n)$, and $d_i(n)$.

III. ACOUSTIC MODELING

To achieve the flexible positioning of the error microphone, the remote adaptive algorithm is implemented in parallel-form NANC system. In the remote adaptive algorithm, the transfer function of the remote controller is derived based on the system model in the acoustic domain. To study the behavior

of the acoustic wave, the homogeneous wave equations are well defined in the literature, but here we need to reformulate these equations in a way we used in our NANC system.

$$\nabla^2 p(x, t) - \frac{1}{c^2} \frac{\partial^2}{\partial t^2} p(x, t) = 0 \quad (11)$$

Equation (11) is a well-known homogeneous acoustic wave equation, where operator ∇^2 is referred as Laplace operator. The wave equation can be described in the frequency domain by applying the Fourier transform of the acoustic pressure and the particle velocity. The Fourier transform pair of the acoustic pressure with respect to the time is given by

$$P(x, \omega) = \mathcal{F}_t\{p(x, t)\} = \int_{-\infty}^{\infty} p(x, t) e^{-j\omega t} dt \quad (12)$$

$$p(x, t) = \mathcal{F}_t^{-1}\{P(x, \omega)\} = \frac{1}{2\pi} \int_{-\infty}^{\infty} P(x, \omega) e^{j\omega t} d\omega \quad (13)$$

where $\omega = 2\pi f$ represents the radial frequency, and $\mathcal{F}_t\{\cdot\}$ describes the Fourier transformation with respect to the time. Updating wave equation (11) by incorporating $P(x, \omega)$ and applying the differentiation theorem of the Fourier transform, formulates the wave equation in the frequency domain.

$$\nabla^2 P(x, \omega) + \left(\frac{\omega}{c}\right)^2 P(x, \omega) = 0 \quad (14)$$

This form of the wave equation is defined as the Helmholtz equation. The term $\frac{\omega}{c}$ denotes the acoustic wave number k .

$$k^2 = \left(\frac{\omega}{c}\right)^2 \quad (15)$$

A. Homogeneous Wave Equation in Spherical Coordinates

In the spherical coordinate system, the Laplace operator ∇^2 used in the wave equation (11) is given as

$$\nabla^2 = \frac{1}{r^2} \frac{\partial}{\partial r} \left(r^2 \frac{\partial}{\partial r} \right) + \frac{1}{r^2 \sin\phi} \frac{\partial}{\partial \phi} \left(\sin\phi \frac{\partial}{\partial \phi} \right) + \frac{1}{r^2 \sin^2\phi} \frac{\partial^2}{\partial \theta^2} \quad (16)$$

where (θ, ϕ, r) denotes the position in spherical coordinate system. The solution of wave equation define in (11) can be expressed as a product of four independent functions of spatial variables (θ, ϕ, r) and time t .

$$p(\theta, \phi, r, t) = p_\theta(\theta) \cdot p_\phi(\phi) \cdot p_r(r) \cdot p_t(t) \quad (17)$$

To separate the (17) into four differential equations in θ, ϕ, r and t , the terms dependent on the respective other three quantities are replaced by a constant, which leads to four differential equations.

$$\frac{1}{c^2} \left(r^2 \frac{\partial p_t(t)}{\partial t^2} \right) + k^2 p_t(t) = 0 \quad (18)$$

$$\frac{\partial^2 p_\phi(\phi)}{\partial \phi^2} + m^2 p_\phi(\phi) = 0 \quad (19)$$

$$\frac{1}{\sin\theta} \frac{\partial}{\partial \theta} \left(\sin\theta \frac{\partial p_\theta(\theta)}{\partial \theta} \right) + \left(n(n+1) - \frac{m^2}{\sin^2\theta} \right) p_\theta(\theta) = 0 \quad (20)$$

$$\frac{1}{r^2} \frac{\partial}{\partial r} \left(r^2 \frac{\partial p_r(r)}{\partial r} \right) + k^2 p_r(r) - \frac{n(n+1)}{r^2} p_r(r) = 0 \quad (21)$$

The solution of (18) with $k = \omega/c$ reads

$$p_t(t) = T_1 e^{-i\omega t} + T_2 e^{+i\omega t} \quad (22)$$

and the solution of (19) is given as

$$p_\phi(\phi) = \Phi_1(m) e^{im\phi} + \Phi_2(m) e^{-im\phi} \quad (23)$$

where T_1, T_2, Φ_1, Φ_2 denote arbitrary constants. The solution of (20) is found using a transformation of variable. Let $\eta = \cos(\theta)$, where $(-1 \leq \eta \leq 1)$ so that the differential equation (Legendre equation) for $p_\theta(\theta)$ becomes

$$\frac{\partial}{\partial \eta} \left((1-\eta^2) \frac{\partial p_\theta(\theta)}{\partial \eta} \right) + \left(n(n+1) - \frac{m^2}{1-\eta^2} \right) p_\theta(\theta) = 0 \quad (24)$$

The solution is given by P_n^m and Q_n^m , Legendre functions of the first and second kind respectively.

$$p_\theta(\theta) = \Theta_1 P_n^m(\cos\theta) + \Theta_2 Q_n^m(\cos\theta) \quad (25)$$

Where Θ_1, Θ_2 denote arbitrary constants. The Legendre functions of the second kind Q_n^m are finite at the poles where $\eta = \pm 1$ so this solution is discarded ($\Theta_2 = 0$).

The radial differential equation (21) can be rewritten as

$$\left(\frac{\partial^2}{\partial r^2} + \frac{2}{r} \frac{\partial}{\partial r} + k^2 - \frac{n(n+1)}{r^2} \right) p_r(r) = 0 \quad (26)$$

which would be Bessel's equation, except for the coefficient of $2/r$ instead of $1/r$. However, with suitable substitution of $p_r(r) = \frac{1}{r^{1/2}} u_r(r)$ (26) can be transformed to Bessel's equation as follows

$$\left(\frac{\partial^2}{\partial r^2} + \frac{1}{r} \frac{\partial}{\partial r} + k^2 - \frac{n(n+1/2)^2}{r^2} \right) u_r(r) = 0 \quad (27)$$

The solution of the above Bessel's differential equation yields

$$p_r(r) = \frac{A_n}{r^{1/2}} J_{n+1/2}(kr) + \frac{B_n}{r^{1/2}} Y_{n+1/2}(kr) \quad (28)$$

where $J_{n+1/2}(\cdot)$ and $Y_{n+1/2}(\cdot)$ are Bessel functions of the first and second kind respectively, and A_n and B_n denote arbitrary constants. Thus, a new form of Bessel functions, so-called spherical Bessel functions of the first and second kind can be defined as follows

$$j_n(x) = \left(\frac{\pi}{2x} \right)^{\frac{1}{2}} J_{n+1/2}(x) \quad (29)$$

$$y_n(x) = \left(\frac{\pi}{2x} \right)^{\frac{1}{2}} Y_{n+1/2}(x) \quad (30)$$

The spherical Hankel functions of the first and second kind are defined in terms of these solutions

$$h_n^{(1)}(x) = j_n(x) + iy_n(x) \quad (31)$$

$$h_n^{(2)}(x) = j_n(x) - iy_n(x) \quad (32)$$

The Hankel functions are combined into a single function called a spherical harmonic Y_n^m defined by

$$Y_n^m(\theta, \phi) = \sqrt{\frac{(2n+1)(n-m)}{4\pi(n+m)}} P_n^m(\cos\theta) e_{im\phi} \quad (33)$$

Thus, any solution as outgoing traveling wave $e^{-i\omega t}$ of (11) can be formulated as

$$P(\theta, \phi, r, \omega) = \sum_{n=0}^{\infty} \sum_{m=-n}^n (A_{mn} j_n(kr) + B_{mn} y_n(kr)) Y_n^m(\theta, \phi) \quad (34)$$

Now, the function defined in (34) is used to find the transfer function of the optimal remote controller in the spherical coordinate system, which creates a zone of quiet at a remote location while the error microphone remains untouched. In a parallel-form narrowband ANC system, the input signal is separated into multiple channels on the bases of frequency components. In this case, the transfer function of an optimal remote controller is derived for each frequency component and work with each independent input signal. The transfer function of optimal remote controller $\widetilde{W}_{opt\ i}(z)$ is defined as

$$\widetilde{W}_{opt\ i}(z) = \rho_i(z) W_{opt\ i}(z) \quad i = 1, 2, \dots, M \quad (35)$$

Where, $\widetilde{W}_{opt\ i}(z)$ is the series combination of the remote controller transfer function $\rho_i(z)$ and traditional ANC controller $W_{opt\ i}(z)$. Where the $\rho_i(z)$ is given by

$$\rho_i(z) = K_{ri} z^{-\Delta_{ri}} \quad (36)$$

Where Δ_{ri} is the time-delay and K_{ri} is the static gain of a remote controller. The complete derivation of time-delay Δ_r and static gain K_r is presented in [17].

IV. PARALLEL FORM NARROWBAND REMOTE ANC

The structure of the proposed parallel-form remote NANC system is shown in Fig. 2. The standard parallel-form active noise control comprises FxLMS as an adaptive algorithm. However, as shown in the figure, our proposed system has a remote controller ρ in each channel. So the adaptive algorithm is modified to indemnify for the effect of a remote controller $\rho_i(z)$. In an adaptive remote algorithm, the reference signal is the same. However, the error signal is different from the error signal of the original FxLMS based system. In the standard FxLMS based NANC system, the error signal in the z-domain is defined as

$$E_i^*(z) = P(z)X_i(z) + W_i(z)S(z)X_i(z) \quad i = 1, 2, \dots, M \quad (37)$$

However, the error signal in remote ANC system can be expressed as:

$$E_i(z) = P(z)X_i(z) + W_i(z)\rho_i(z)S(z)X_i(z) \quad i = 1, 2, \dots, M \quad (38)$$

so, the difference between error signals can be obtained by subtracting (37) from (38).

$$\Delta E_i(z) = E_i^*(z) - E_i(z) \quad (39)$$

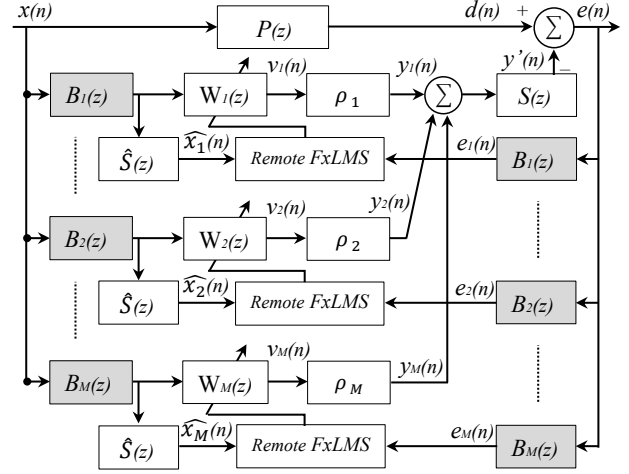


Fig. 2: Block diagram of parallel-form remote ANC

$$\Delta E_i(z) = W_i(z)S(z)X_i(z) - W_i(z)\rho_i(z)S(z)X_i(z) \quad (40)$$

As shown in Fig. 2, (40) can be simplified as

$$\Delta E_i(z) = S(z)Y_i(z) - Y_{ri}(z) \quad (41)$$

$\Delta E_i(z)$, in time domain can be expressed as

$$\Delta e_i(n) = s(n) * \{y_i(n) - y_{ri}(n)\} \quad (42)$$

$\Delta e_i(n)$ is the difference between the remote ANC error signal and the desired error signal. So, the $\Delta e_i(n)$ should be added to $e_i(n)$ in updating the error signal to compensate for the influence of a remote controller. The resultant updated remote FxLMS algorithm can be expressed as

$$\mathbf{w}_i(n+1) = \mathbf{w}_i(n) + \mu_i \{e_i(n) + \Delta e_i(n)\} \hat{\mathbf{x}}_i(n) \quad (43)$$

Where, \mathbf{w}_i is the weight vector of length L to represent the impulse response coefficient W and μ_i is adaption step-size.

$$\mathbf{w}_i(n) = [w_{i,0}(n) \ w_{i,1}(n) \ \dots \ w_{i,L-1}(n)]^T \quad (44)$$

and

$$\hat{\mathbf{x}}_i(n) = \hat{s}_i(n) * \mathbf{x}_i(n) \quad (45)$$

$\hat{\mathbf{x}}_i(n)$ is the filtered reference signal of the input $x_i(n)$. Where $\hat{s}_i(n)$ is the estimated impulse response of the secondary path S_i , and $\mathbf{x}_i(n)$ is the input signal vector defined as

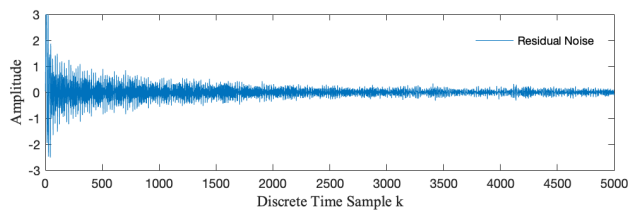
$$\mathbf{x}_i(n) = [x_i(n) \ x_i(n-1) \ \dots \ x_i(n-L+1)]^T \quad (46)$$

Consequently, the remote FxLMS algorithm updates the adaptive weight vector W_i by (43) and computes a control signal $y_i(n)$ as

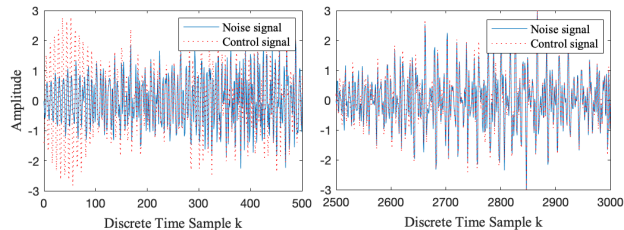
$$y_i(n) = \sum_{l=0}^{L-1} w_{i,l}(n)x_i(n-l) = \mathbf{w}_i^T(n)\mathbf{x}_i(n) \quad (47)$$

The canceling signal $y(n)$ is a combination of the M adaptive filters.

$$y(n) = \sum_{i=1}^M y_i(n) \quad (48)$$



(a) Residual noise at remote ZoQ location



(b) System adaptation at discrete samples (0-500 & 2500-3000)

Fig. 3: Parallel-form multi-tonal remote ANC

The control signal $y(n)$ is used to derive the secondary noise in an acoustic domain. Then, the superposition of primary and secondary sound fields cancel out each other through destructive interference and creates a ZoQ at a remote location rather than the location of an error microphone.

V. SIMULATION RESULTS

In order to show the validity of the proposed algorithm, a set of computer simulation experiments has been performed. In the following simulation experiments, the proposed parallel-form remote ANC system is implemented on a set of the Bark frequency spectrum, and target the central Bark frequency in each critical band from (100-600) Hz. The delayless bandpass filters are used to separate the frequencies into five parallel adaptive filters. In this case, each adaptive filter works independently with a single frequency component and its corresponding remote adaptive controller ρ . Then the output of all adaptive filters summed together to produce a single anti-noise. The updated remote FxLMS can adaptively get an estimate of W_{opt} at the presence of ρ in the control system. Although the bandpass filters do not bring any additional phase shift at the targeted frequency, it has a transient effect, and it does introduce an additional group delay into the secondary path as discussed in [18]. To overcome this effect, the filter-bank must reach the steady-state before performing the secondary path estimation.

In the simulation experiments, the Bark frequency spectrum consists of five Bark frequencies (150, 250, 350, 450, 570) Hz. So, the five bandpass IIR filters, $B_M(z)$, $M = 1, 2, 3, 4, 5$ are centered at corresponding frequencies to split the frequency component of input and error signals. The simulation results of parallel-form remote NANC system are shown in Fig. 3. Where Fig. 3(a) shows the residual noise at the desired remote location and Fig. 3(b) demonstrate the adaptation of the proposed system at a different set of discrete samples (0 – 500) and (2500 – 3000). In order to study the response

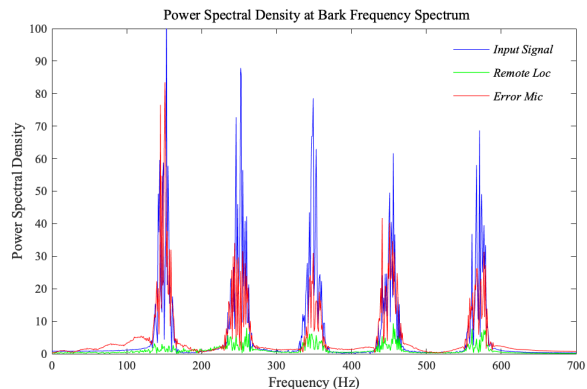


Fig. 4: Power Spectral Density at Bark frequency spectrum

of the proposed system at each frequency component, the graph shown in Fig. 4 offers the compelling analysis by using a power spectral density function. In this graph, the signal shown in blue color is the power of the input noise signal for the complete spectrum. The signal shown in red color is the residual noise measured at the physical error microphone. In contrast, the signal in green color shows the power of residual noise at the desired remote location, which is significantly reduced and exhibits the overall performance of the proposed system.

The results shown in Fig. 5 leads to a similar conclusion and validates that the proposed algorithm performs substantially better at a remote location rather than the location of the physical error microphone. The frequency Fourier transform method is used to analysis each individual frequency of the Bark frequency spectrum. Fig. 5(a) shows the input signals of the Bark frequency spectrum, while Fig. 5(b) shows the residual noise at an error microphone of parallel form remote NANC system. In Fig. 5(c) the resultant noise shows the 20dB noise reduction at the desired remote location. Therefore, these results show that the proposed structure is potentially feasible for many industrial and automotive narrowband applications where there are physical and application constraints to achieve the noise attenuation at the desired location.

VI. CONCLUSIONS

Conventional parallel-form ANC systems are only able to make a zone of quiet at the location of an error microphone. In the single-channel ANC system, it is usually small and occupied by the error microphone itself. Moreover, in many industrial and automotive applications, there are physical limitations and application constraints to place an error microphone at the desired location. In this paper, we have developed a novel parallel-form remote ANC algorithm to create a zone of quiet (ZoQ) at the desired location, remote to the physical error microphone. Taking the human auditory principle into account, the proposed algorithm is implemented on a set of the Bark frequency spectra. In the parallel-form ANC system the signal is forwarded to a series of adaptive filters. Each adaptive filter works independently with a single frequency component

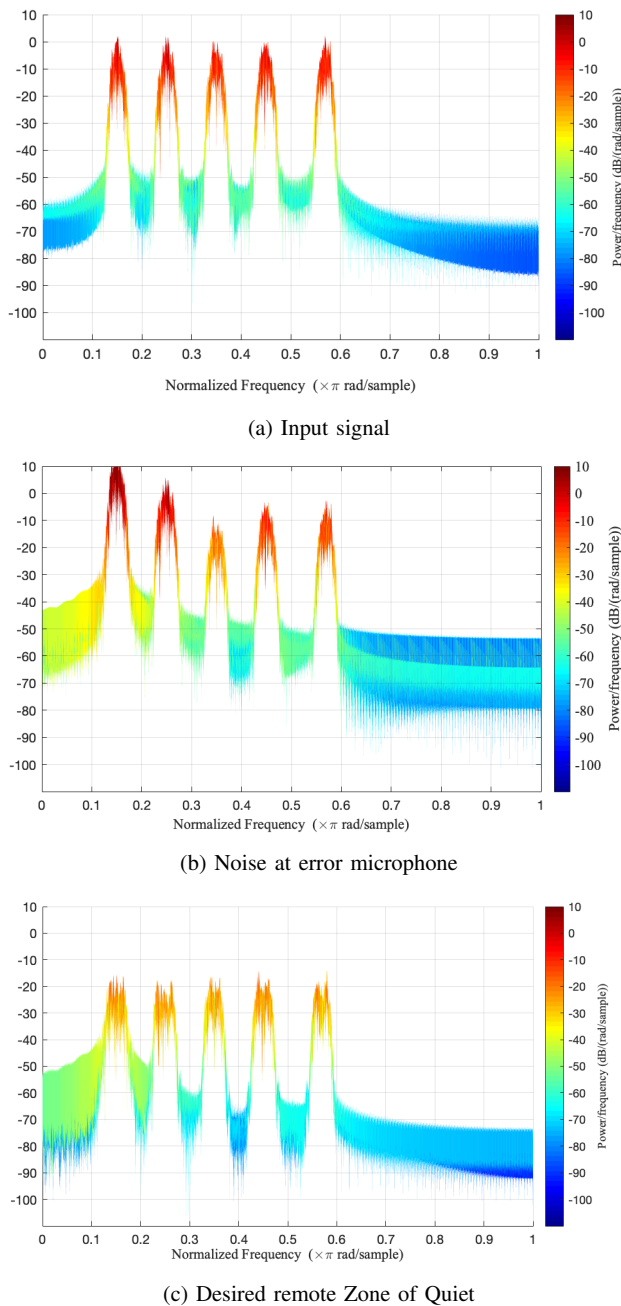


Fig. 5: FFT of parallel form remote ANC (a) Input noise signal, (b) Noise at error microphone, (c) Remote ZoQ

and its corresponding remote adaptive controller. The transfer function of the remote adaptive controller for each frequency component is derived through the wave equation in the acoustic domain. The simulation results based on the remote transfer function show that the proposed system is good enough to create a remote ZoQ at a reasonable distance from an error microphone. Moreover, the simulation results demonstrate that the proposed algorithm achieves better noise reduction at the remote region as compared to the physical error microphone

and it can compensate the inherently introduced group delay in the secondary path. As a next step the proposed model has to be tested on the other auditory filter banks and psychoacoustic parameters.

REFERENCES

- [1] S. M. Kuo, and A.B. Puvvala, "Effects of frequency separation in periodic active noise control systems," *IEEE Transactions on Audio, Speech, and Language Processing*, vol. 14, no. 5, pp. 1857-1866, 2006.
- [2] Y. Xiao, A. Ikuta, L. Ma, and K. Khorasani, "Stochastic Analysis of the FXLMS-Based Narrowband Active Noise Control System," *IEEE Transactions on Audio, Speech, and Language Processing*, vol. 16, no. 5, pp. 1000-1014, 2008.
- [3] F. Yang, A. Gupta, and S. Kuo, "Analysis of narrowband active noise and vibration control systems using parallel adaptive notch filters," *Journal of Vibration and Control*, vol. 14, no. 7, pp. 931-951, 2008.
- [4] F. Yang, A. Gupta, and S. M. Kuo, "Parallel multi-frequency narrowband active noise control systems," *2009 IEEE International Conference on Acoustics, Speech and Signal Processing*, 2009: IEEE, pp. 253-256.
- [5] Y. Pasco, O. Robin, P. Bélanger, A. Berry, and S. Rajan, "Multi-input multi-output feedforward control of multi-harmonic gearbox vibrations using parallel adaptive notch filters in the principal component space," *Journal of sound and vibration*, vol. 330, no. 22, pp. 5230-5244, 2011.
- [6] Y. Xiao, "A New Efficient Narrowband Active Noise Control System and its Performance Analysis," *IEEE Transactions on Audio, Speech, and Language Processing*, vol. 19, no. 7, pp. 1865-1874, 2011.
- [7] C. Chang and S. M. Kuo, "Complete Parallel Narrowband Active Noise Control Systems," *IEEE Transactions on Audio, Speech, and Language Processing*, vol. 21, no. 9, pp. 1979-1986, 2013.
- [8] C. Chang and S. M. Kuo, "Complete direct/parallel structure for narrowband active noise control systems," *IET Signal Processing*, vol. 7, no. 6, pp. 477-485, 2013.
- [9] J. Li, S. M. Kuo, and C. Chang, "Splitting frequency components of error signal in narrowband active noise control system design," *2013 Asia-Pacific Signal and Information Processing Association Annual Summit and Conference*, 29 Oct. 2013, pp. 1-6.
- [10] B. Huang, L. Wen, Y. Xiao, J. Sun, and Y. Shen, "A complete parallel narrowband active noise control system based on residual error separation using variable leaky LMS," *2015 Asia-Pacific Signal and Information Processing Association Annual Summit and Conference (APSIPA)*, 16-19 Dec. 2015, pp. 981-985.
- [11] C. Chang, S. M. Kuo, and A. Siswanto, "Enhanced offline secondary path modeling method for narrowband active noise control system," *39th International Conference on Telecommunications and Signal Processing (TSP)*, 27-29 June 2016, pp. 307-310.
- [12] D. Moreau, B. Cazzolato, A. Zander, and C. Petersen, "A Review of Virtual Sensing Algorithms for Active Noise Control," *Algorithms*, vol. 1, no. 2, 2008, doi: 10.3390/a1020069.
- [13] D. P. Das, D. J. Moreau, and B. S. Cazzolato, "A computationally efficient frequency-domain filtered-X LMS algorithm for virtual microphone," *Mechanical Systems and Signal Processing*, vol. 37, pp. 440-454, 2013.
- [14] S. J. Elliott, W. Jung, and J. Cheer, "Causality and Robustness in the Remote Sensing of Acoustic Pressure, with Application to Local Active Sound Control," *ICASSP 2019 - 2019 IEEE International Conference on Acoustics, Speech and Signal Processing (ICASSP)*, 12-17 May 2019 2019, pp. 8484-8488.
- [15] M. W. Munir, W. H. Abdulla, and I. T. Ardekani, "Psychoacoustically Motivated Active Noise Control at Remote Locations," *2019 Australian & New Zealand Control Conference (ANZCC)*, 27-29 Nov. 2019, pp. 72-75.
- [16] C. Shi, R. Xie, N. Jiang, H. Li, and Y. Kajikawa, "Selective Virtual Sensing Technique for Multi-channel Feedforward Active Noise Control Systems," *2019 IEEE International Conference on Acoustics, Speech and Signal Processing (ICASSP)*, 12-17 May 2019 2019, pp. 8489-8493.
- [17] I. T. Ardekani and W. H. Abdulla, "An adaptive signal processing system for active control of sound in remote locations," *2013 Asia-Pacific Signal and Information Processing Association Annual Summit and Conference*, 29 Oct.-1 Nov. 2013, pp. 1-7, doi: 10.1109/APSIPA.2013.6694322.
- [18] J. Cheer and S. J. Elliott, "Comments on "Complete Parallel Narrowband Active Noise Control Systems", *IEEE/ACM Transactions on Audio, Speech, and Language Processing*, vol. 22, no. 5, pp. 995-996, 2014.